

# The Chromospheric Field Probed by the He I 10830 Line

## Some Recent Developments

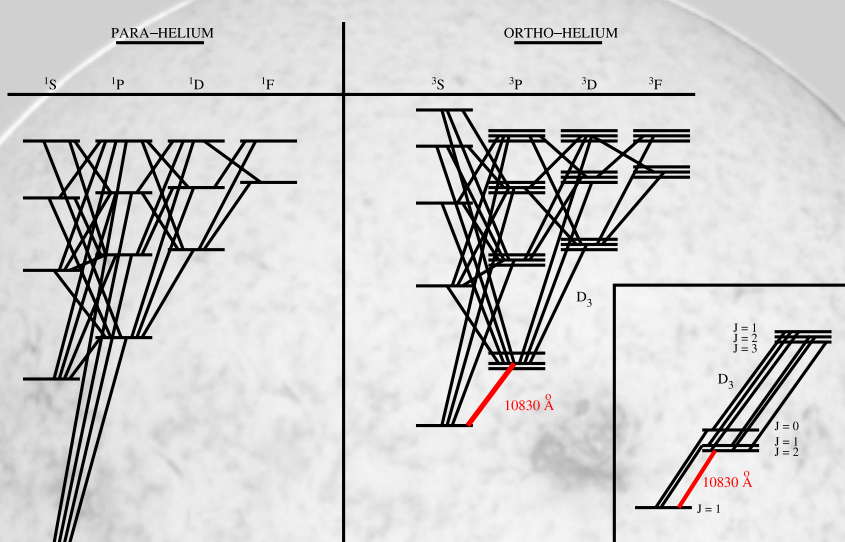
Andreas Lagg

Max-Planck-Institut für Sonnensystemforschung  
Göttingen, Germany

Coupling and Dynamics of the Solar Atmosphere  
Pune, India  
Nov-11 2014



## The He I atom (Centeno et al., 2008)

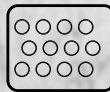


## Coronal Illumination - Ionization - Recombination (Centeno et al., 2008)

(1) No CI

He II

He I

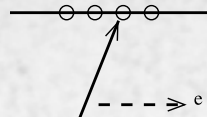
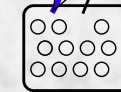


SINGLETS



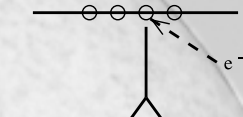
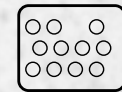
TRIPLETS

(2) ionization

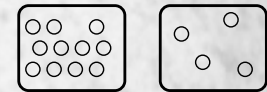


$e^-$

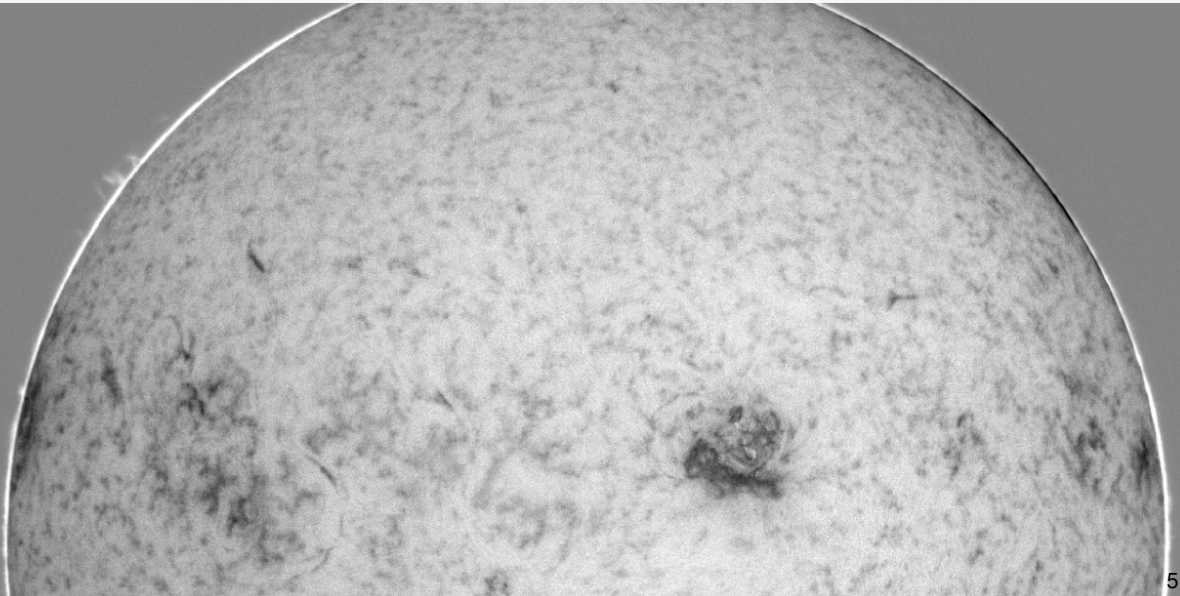
(3) recombination



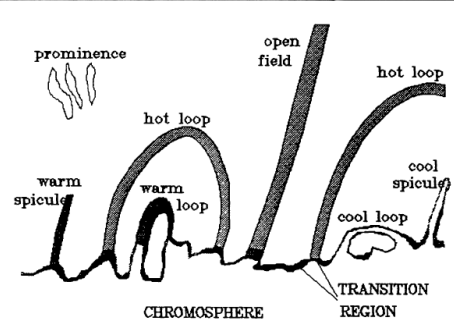
$e^-$



## He I – What can be observed?

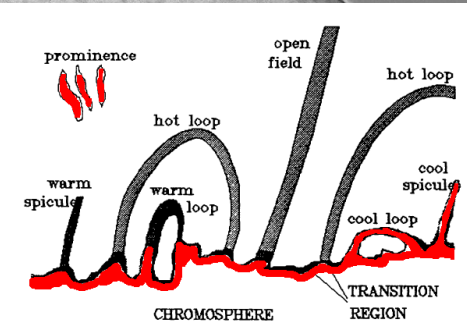


## He I – Formation Height



Avrett et al. (1994)

## He I – Formation Height



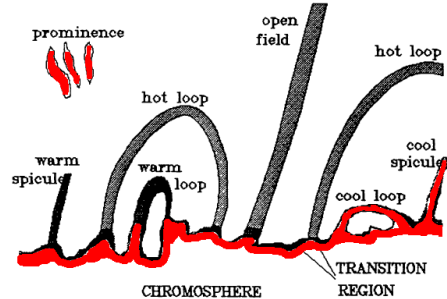
Avrett et al. (1994)

## He I – Formation Height

Poster on He D3 results:

T. E. L. Libbrecht et al.:

Spectrographic Helium D3  
observations with SST/TRIPPEL



Avrett et al. (1994)

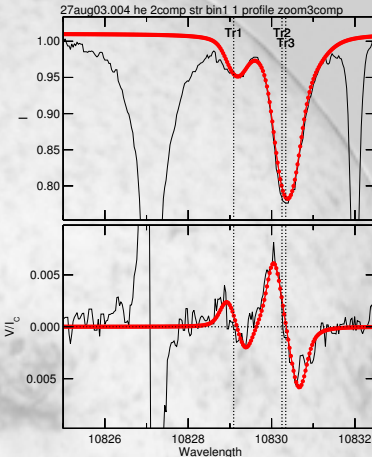
## B-Field and He I 10830 Å

### Zeeman + PB effect

- reliable magnetic field information for  $B > 200$  G
- simultaneous observation of photosphere (Si, Ca) and chromosphere (He)
- three (blended) HeI lines: ("blue" line + 2 "red" lines)
- Paschen-Back effect for stronger fields

### Hanle effect

- sensitive regime:  $\approx 0.1\text{--}8$  G
- saturated regime (8–100 G): directional information



## He I Observatories

### He I 10830 full disk instruments

- SOLIS VSM and FDP  
(NSO; until 2014: Kitt Peak, 2014:  
Tucson: 2015: ???; Keller et al.,  
2003)
- Chrotel  
(KIS; Tenerife; Bethge et al., 2011)
- CHIP  
(MacQueen et al., 1998)
- NAOJ Solar Flare Telescope  
(NAOJ; Hanaoka et al., 2011)

### He I 10830 at high resolution

- TIP-1  
(IAC; Tenerife; Martínez Pillet et al., 1999;  
Collados et al., 1999)
- TIP-2  
(IAC/MPS; Tenerife; Collados et al., 2007)
- ProMag (prominences)  
(NSO; Sunspot; Elmore et al., 2008)

### Recent hi-res Spectropolarimeters

- FIRS, SPINOR, NIRIS, GRIS

## Recent Hi-Res Spectropolarimeters

### SPINOR @ DST (Sac Peak)

Socas-Navarro et al. (2006)

- full Stokes simultaneous obs. of several VIS + IR regions
- virtually any combination of spectral line

### FIRS @ DST (Sac Peak)

Jaeggli et al. (2010); Schad (2013)

- 4-slit, dual-beam spectropol.
- Fe I 630.2 & He I 1083
- simultaneous with IBIS

### NIRIS @ 1.6m NST (Big Bear)

Cao et al. (2012)

- attached to 1.6 m NST at Big Bear
- dual Fabry-Pérot Interferometers
- imaging polarimetry @ 0''.25

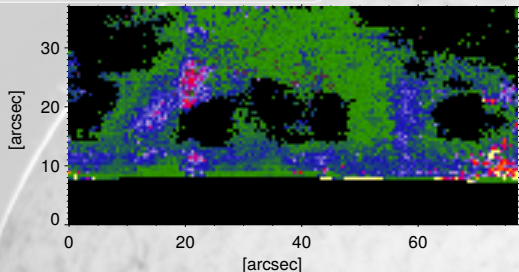
### GRIS @ 1.5m GREGOR (Tenerife)

Collados et al. (2012)

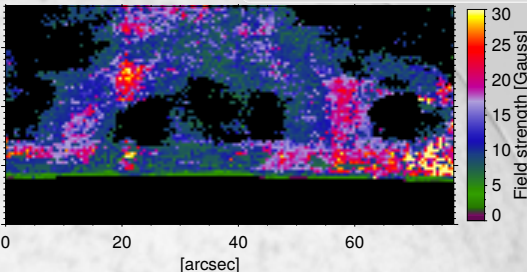
- attached to 1.5 m GREGOR telescope (Tenerife)
- standard Czerny-Turner config.
- spectro-polarimetry @ 0''.25

# The magnetic field configuration of a solar prominence inferred from spectropolarimetric observations in the He I 10830 Å triplet (Orozco Suárez et al., 2014)

quasi-horizontal solution



quasi-vertical solution



HAZEL inversions (Asensio Ramos et al., 2008)

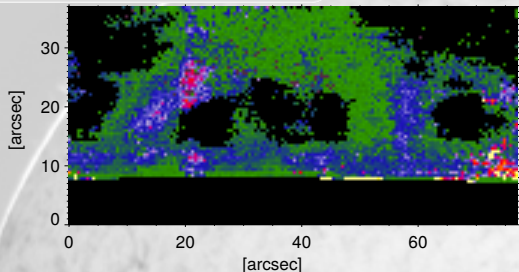
70 s/slit pos

Ambiguities (unresolved, plausibility argument: use quasi-horizontal solution):

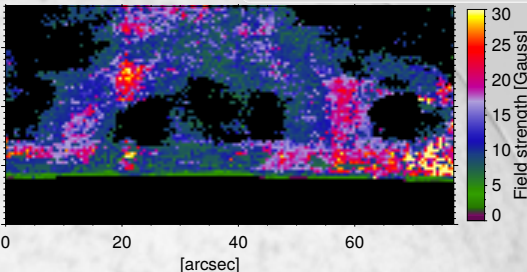
- Zeeman effect:  $180^\circ$  ambiguity
- Hanle effect:  $90^\circ$  and  $180^\circ$  ambiguity

# The magnetic field configuration of a solar prominence inferred from spectropolarimetric observations in the He I 10830 Å triplet (Orozco Suárez et al., 2014)

quasi-horizontal solution



quasi-vertical solution

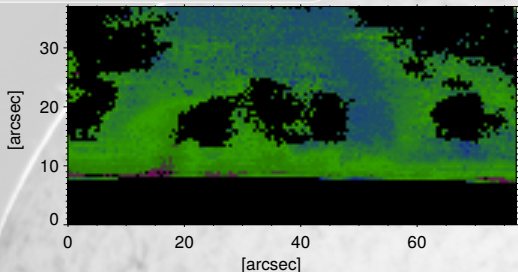


## Magnetic field strength

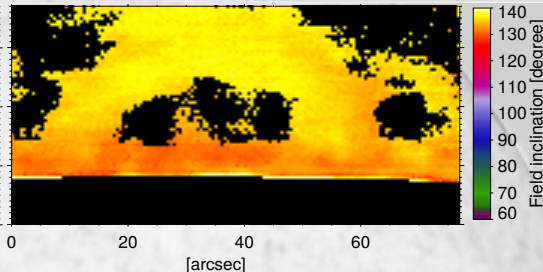
- quiescent prominence, on average 7 G
- up to 30 G at prominence feet (coinciding with high opacity)

# The magnetic field configuration of a solar prominence inferred from spectropolarimetric observations in the He I 10830 Å triplet (Orozco Suárez et al., 2014)

quasi-horizontal solution



quasi-vertical solution

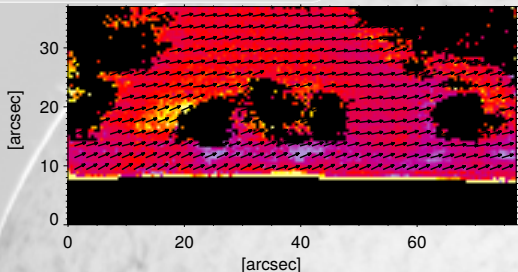


## Magnetic field inclination

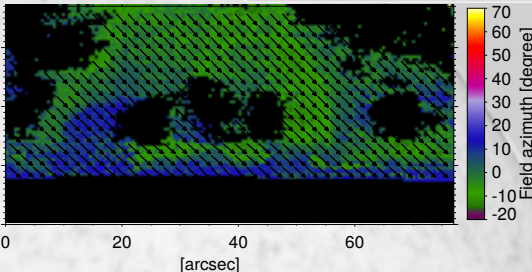
- inclined  $\approx 77^\circ$  to solar vertical;  
in between previous results:  $60^\circ$  (e.g., Bommier et al., 1994) and horizontal  
(Casini et al., 2003)

The magnetic field configuration of a solar prominence inferred from spectropolarimetric observations in the He I 10830 Å triplet (Orozco Suárez et al., 2014)

quasi-horizontal solution



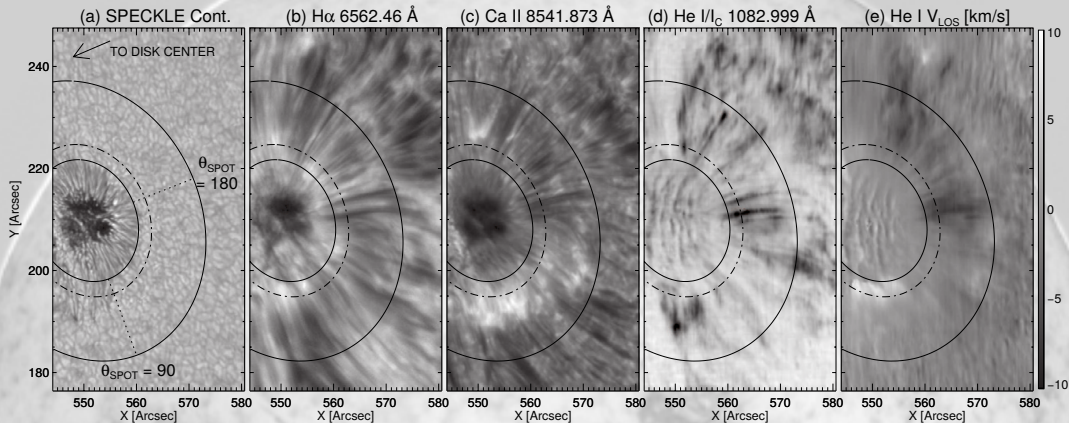
quasi-vertical solution



### Magnetic field orientation wrt. prominence axis

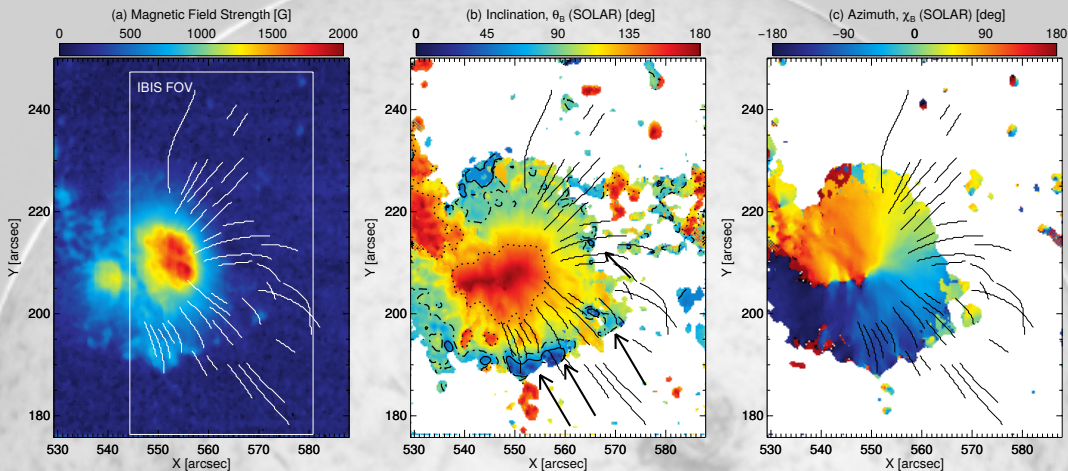
- inclined  $\approx 58^\circ$  /  $\approx 156^\circ$  to prominence long axis  
(unresolved ambiguity), both solutions: inverse polarity prominence

## He I Vector Magnetometry of Field-aligned Superpenumbral Fibrils (Schad et al., 2013)



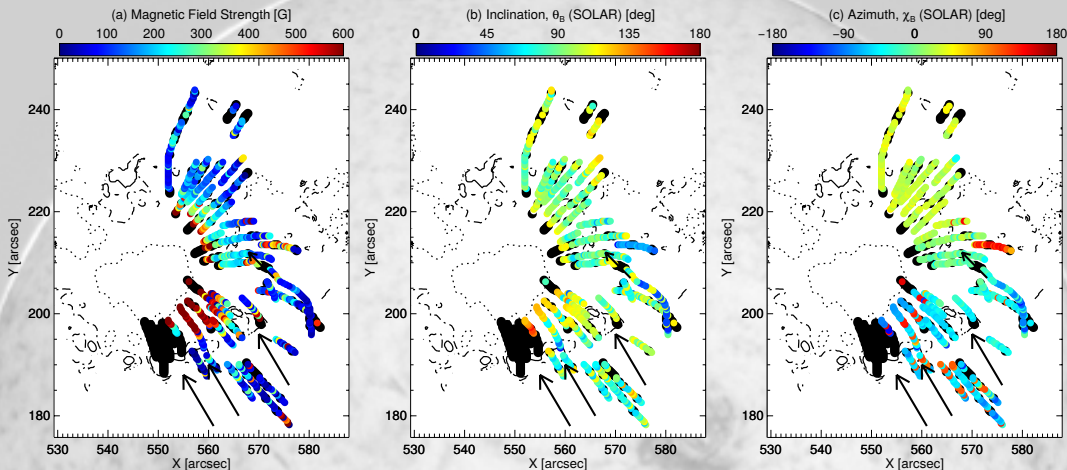
IBIS & FIRS Observations, NOAA AR 11408, Jan 29 2012,  $\mu = 0.8$

## He I Vector Magnetometry of Field-aligned Superpenumbral Fibrils (Schad et al., 2013)



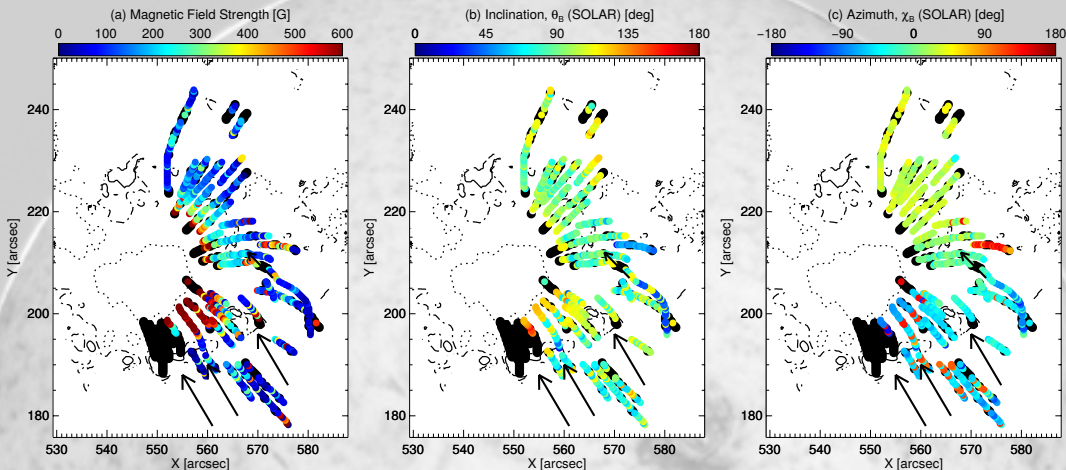
Photospheric field from Si I ME-inversions (HELIx+ Lagg et al., 2009)

## He I Vector Magnetometry of Field-aligned Superpenumbral Fibrils (Schad et al., 2013)



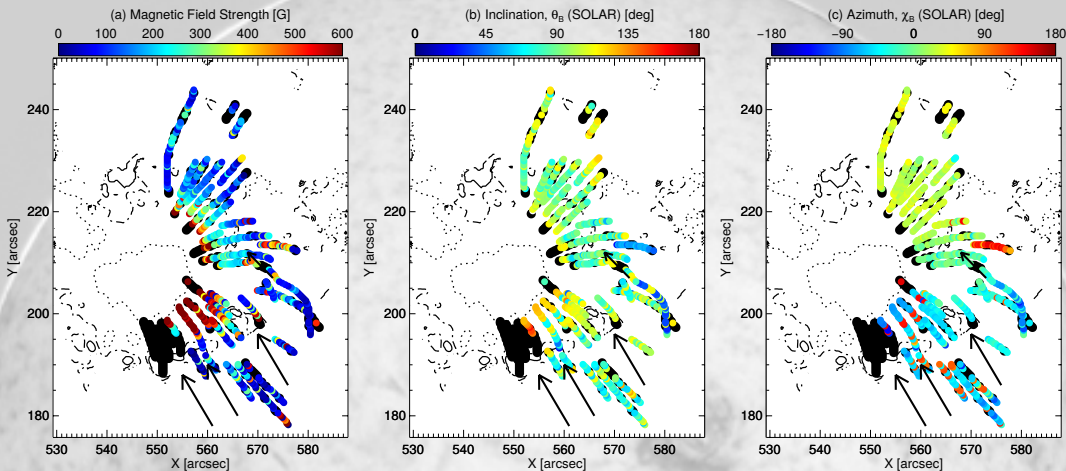
Fibril tracing (CRISPEX, Vissers & Rouppe van der Voort, 2012), careful disambiguation (Hanle & Zeeman), assumption on fibril height (1.75 Mm)

## He I Vector Magnetometry of Field-aligned Superpenumbral Fibrils (Schad et al., 2013)



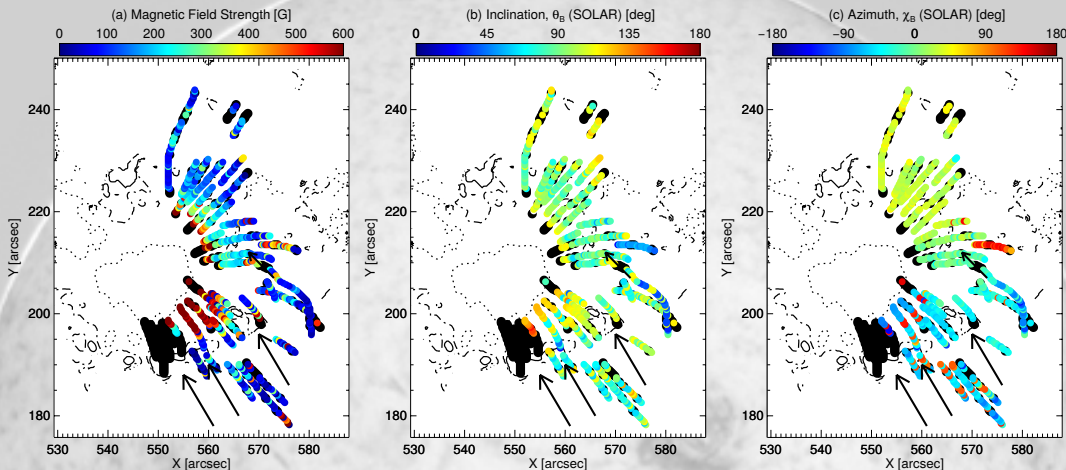
B-strength: rise in strength towards inner endpoints

## He I Vector Magnetometry of Field-aligned Superpenumbral Fibrils (Schad et al., 2013)



B-inclination: change at inner endpoint towards sunspot

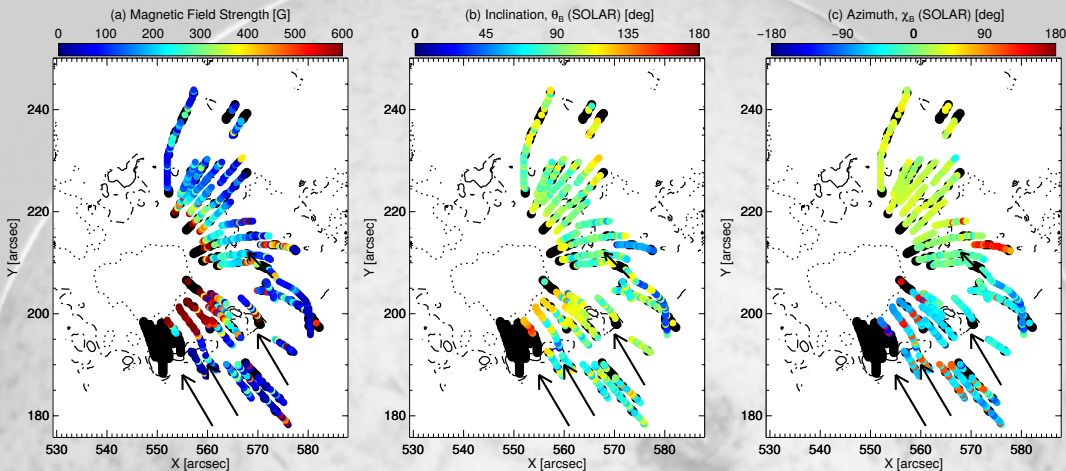
## He I Vector Magnetometry of Field-aligned Superpenumbral Fibrils (Schad et al., 2013)



B-inclination: remain horizontal until outer endpoint

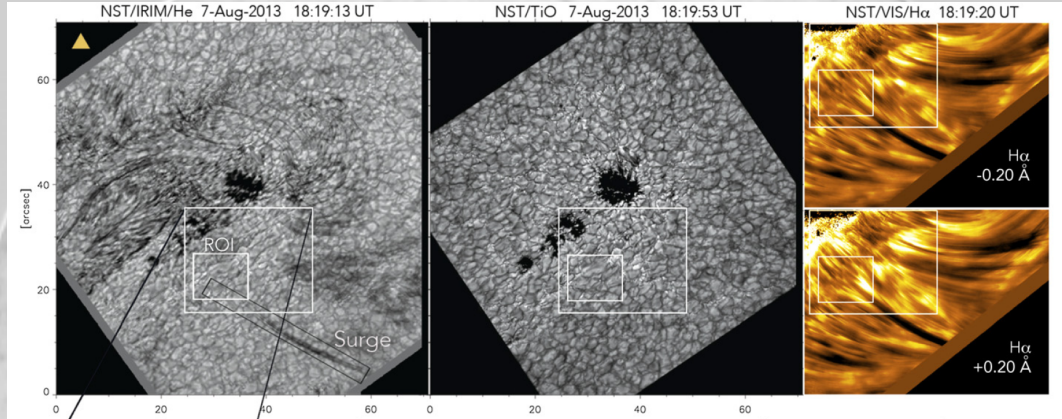
few fibrils: turn over again, connect in regions of opposite polarity photosphere

## He I Vector Magnetometry of Field-aligned Superpenumbral Fibrils (Schad et al., 2013)



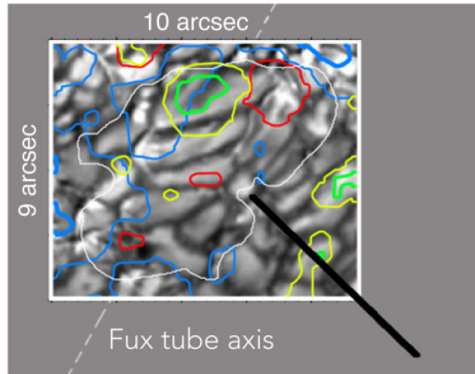
B-azimuth: aligned  $\pm 10^\circ$  with fibrils

# Multi-wavelength High-resolution Observations of a Small-scale Emerging Magnetic Flux Event and the Chromospheric and Coronal Response (Vargas Domínguez et al., 2014)



# Multi-wavelength High-resolution Observations of a Small-scale Emerging Magnetic Flux Event and the Chromospheric and Coronal Response (Vargas Domínguez et al., 2014)

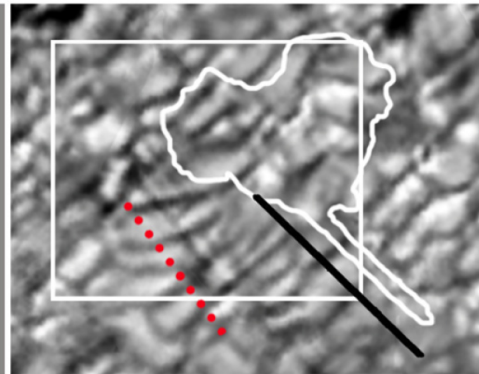
TiO 18:09:45



Magnetic Field  
Doppler Velocity

+	-
Up	Down

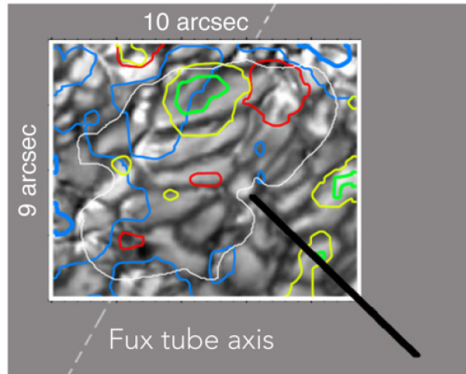
▲ IRIM/He I 18:09:46



white IRIS contour

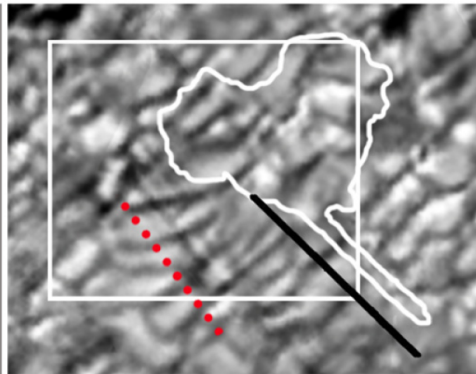
# Multi-wavelength High-resolution Observations of a Small-scale Emerging Magnetic Flux Event and the Chromospheric and Coronal Response (Vargas Domínguez et al., 2014)

TiO 18:09:45



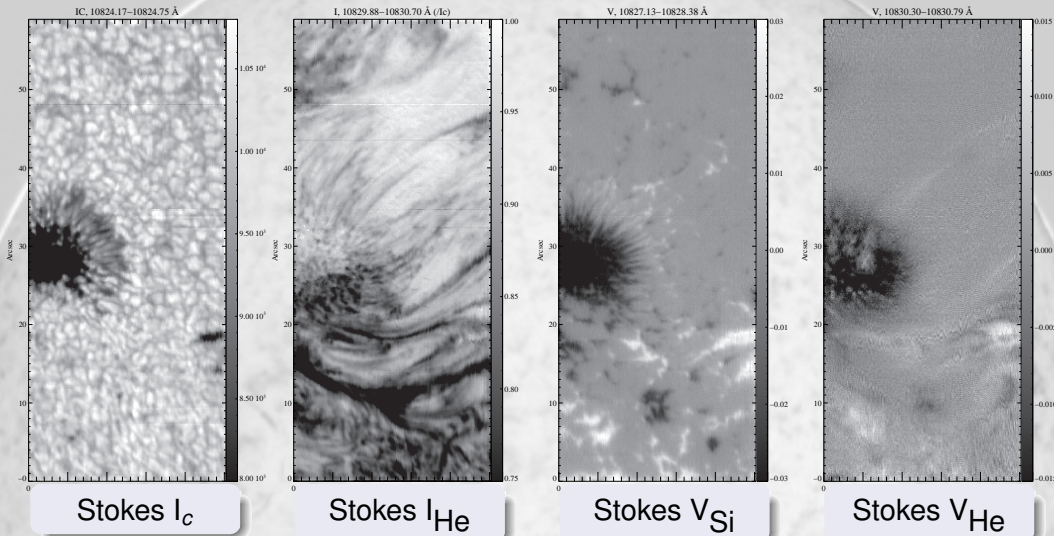
Magnetic Field  
Doppler Velocity + Up - Down

▲ IRIM/He I 18:09:46

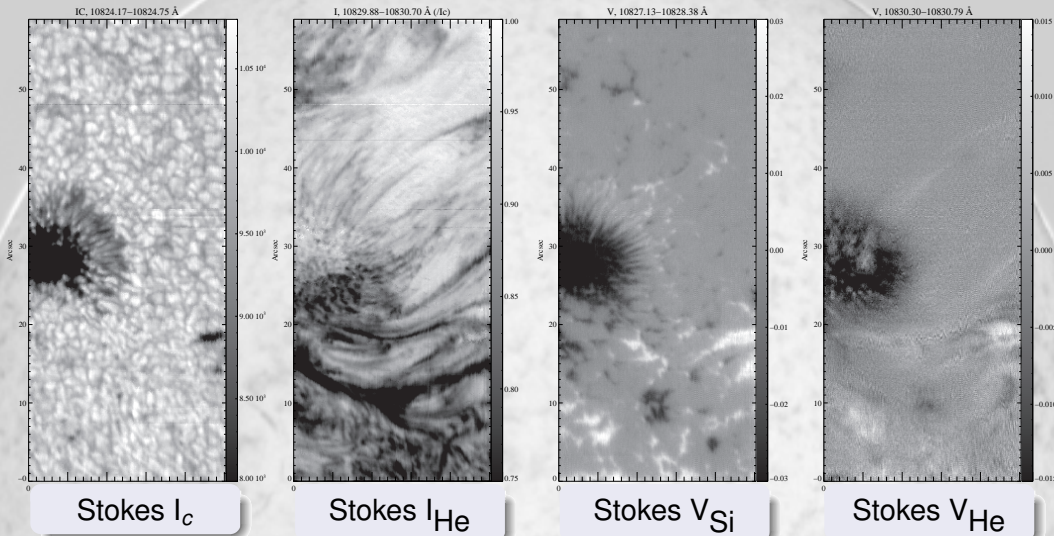


Ubiquitous small-scale reconnection scenario (Shibata et al., 2007)?

## GREGOR/GRIS Data &amp; First Results (June 2014)



## GREGOR/GRIS Data &amp; First Results (June 2014)



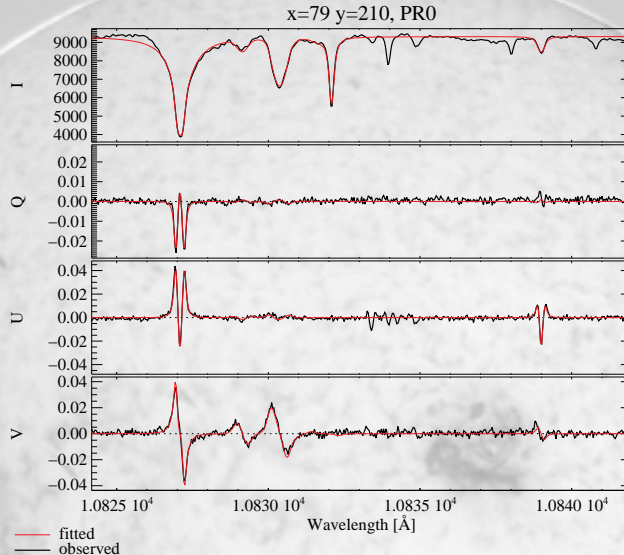
## GREGOR/GRIS Data &amp; First Results (June 2014)

spatial resolution:  $\approx 0.^{\prime\prime}40$   
(diff. limit:  $0.^{\prime\prime}25$ )  
pol. noise level in 5 s:  $5 \cdot 10^{-4} I_C$

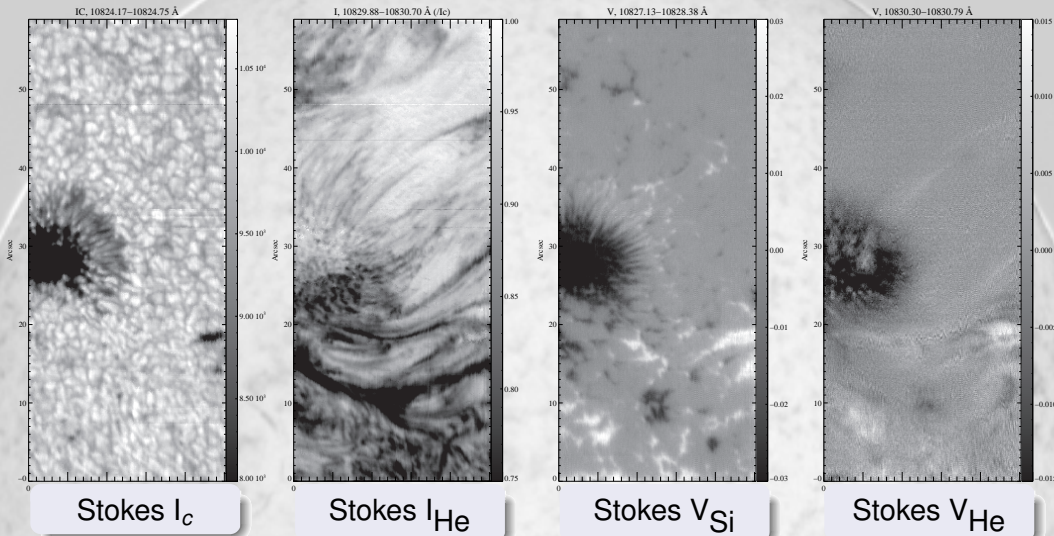
$9.00 \cdot 10^3$

20

## GREGOR/GRIS Data &amp; First Results (June 2014)

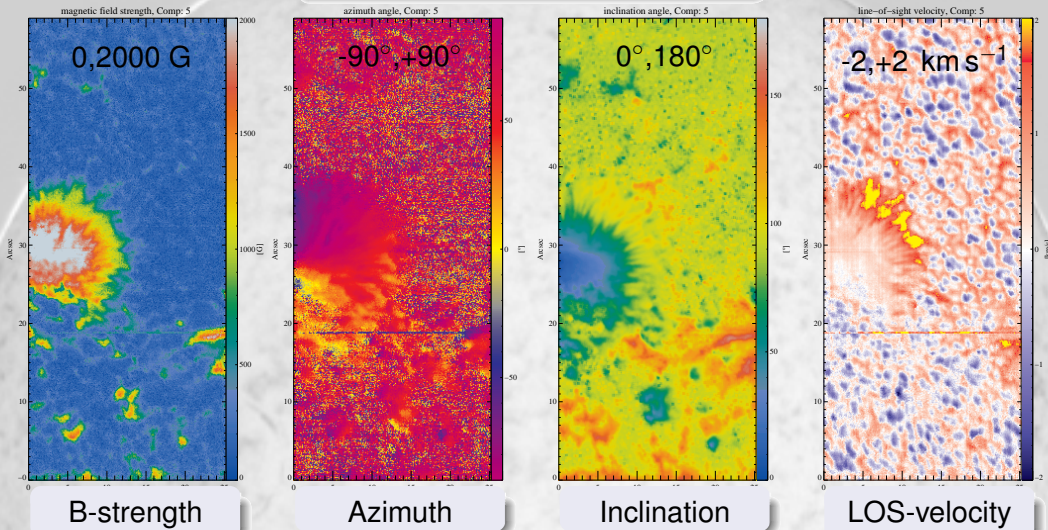


## GREGOR/GRIS Data &amp; First Results (June 2014)



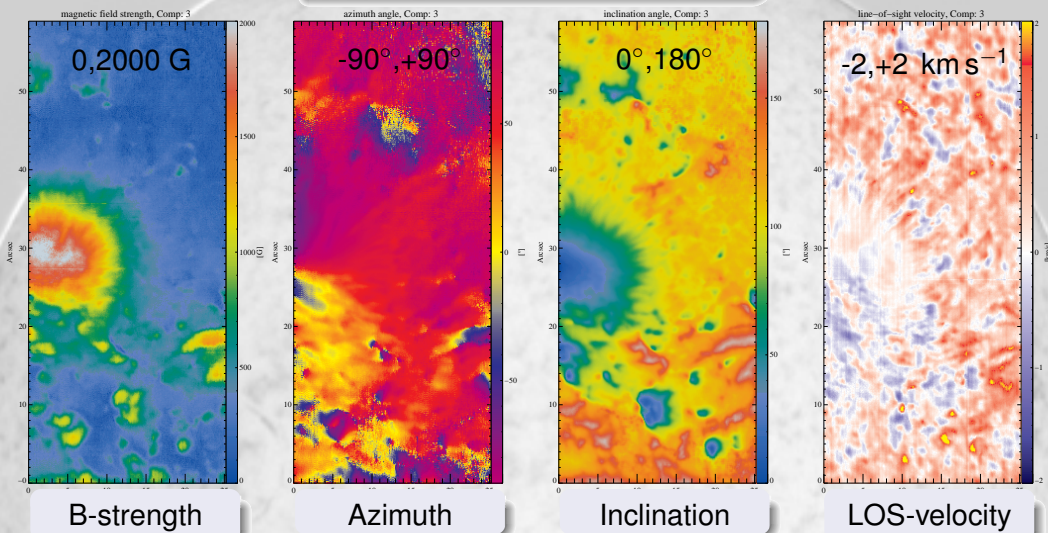
## GREGOR/GRIS Data &amp; First Results (June 2014)

## Ca I – deep photosphere



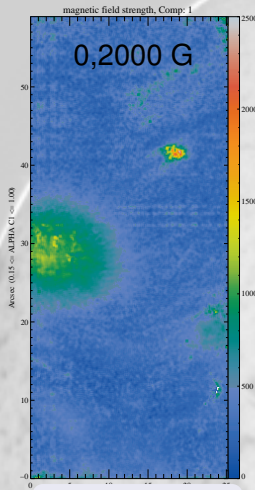
## GREGOR/GRIS Data &amp; First Results (June 2014)

Si I – mid/upper photosphere

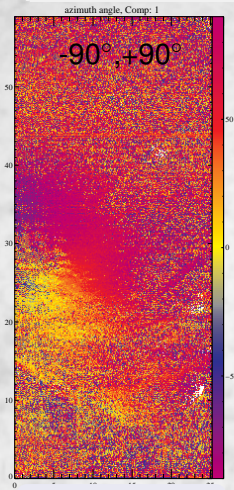


## GREGOR/GRIS Data &amp; First Results (June 2014)

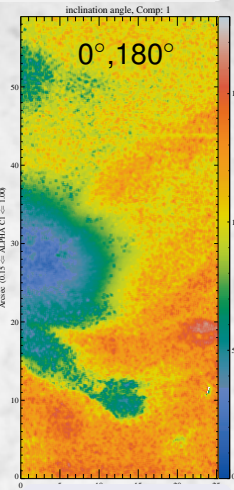
## He I – upper chromosphere



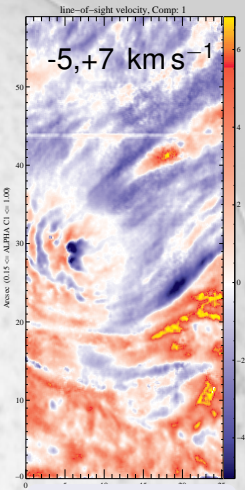
B-strength



Azimuth



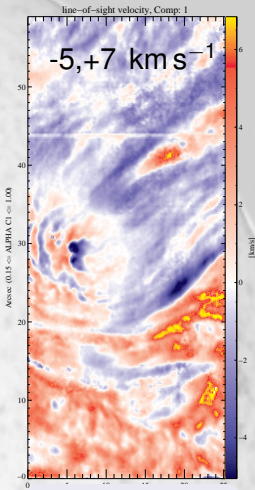
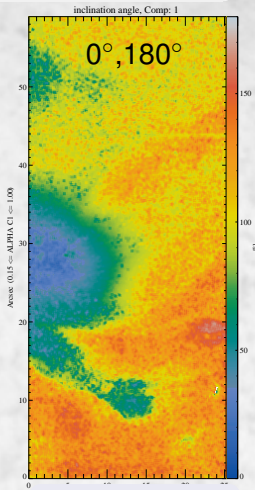
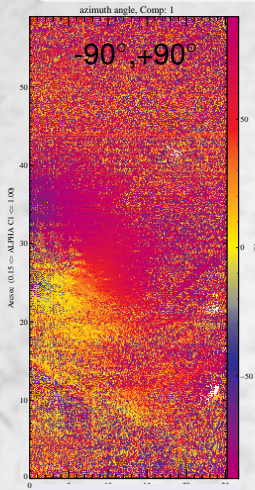
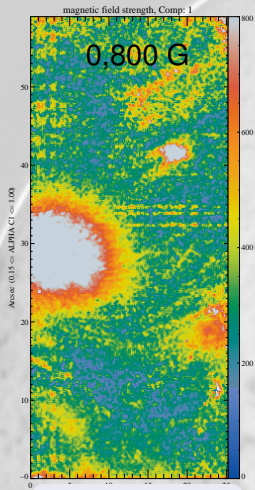
Inclination



LOS-velocity

## GREGOR/GRIS Data &amp; First Results (June 2014)

## He I – upper chromosphere



B-strength

Azimuth

Inclination

LOS-velocity

## Chromospheric Fine Structure: Summary

### Fine structure in the He I spectral region

- fine structure mainly He I intensity:
  - almost absent in Stokes images / B-vector
  - outlines velocity and density/temp. structure
- continuous decrease of fine structure in B with height:

● Ca I (deep photosphere):	0."/40
● Si I (mid/upper photosphere):	0."/70
● He I (chromosphere):	1."/00

## Ground-based: DKIST & NLST

**DL-NIRSP (The Diffraction Limited Near-Infrared Spectropolarimeter, DKIST; Haosheng Lin)**

Spectral Range:

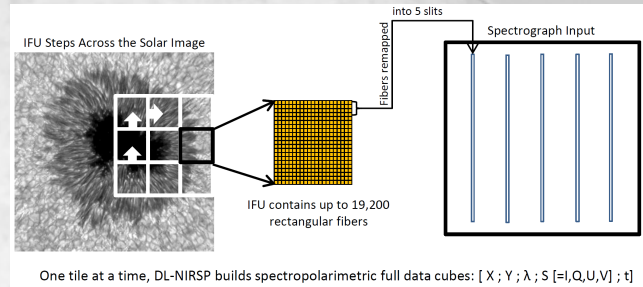
500 nm to 1800 nm

Spectral resolution: up to 250000

Spatial resolution: 0.07'' @10830Å

Target polarimetric accuracy:

$$> 5 \cdot 10^{-4} I_c$$



## NLST @ Hanle, India

Spectropolarimeter:

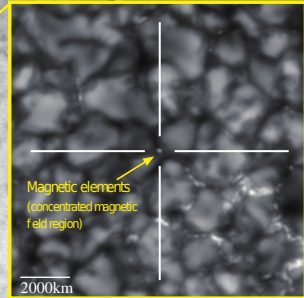
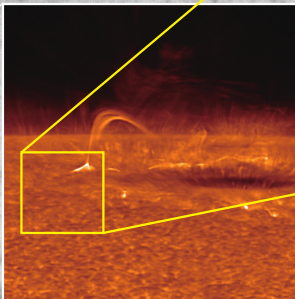
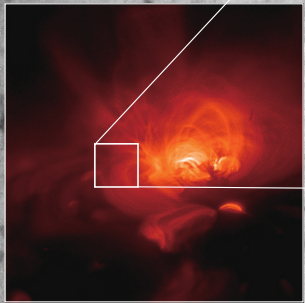
Based on SPINOR design

Spectral Range:

500 nm to 1600 (5000) nm



## Space-borne: Solar-C



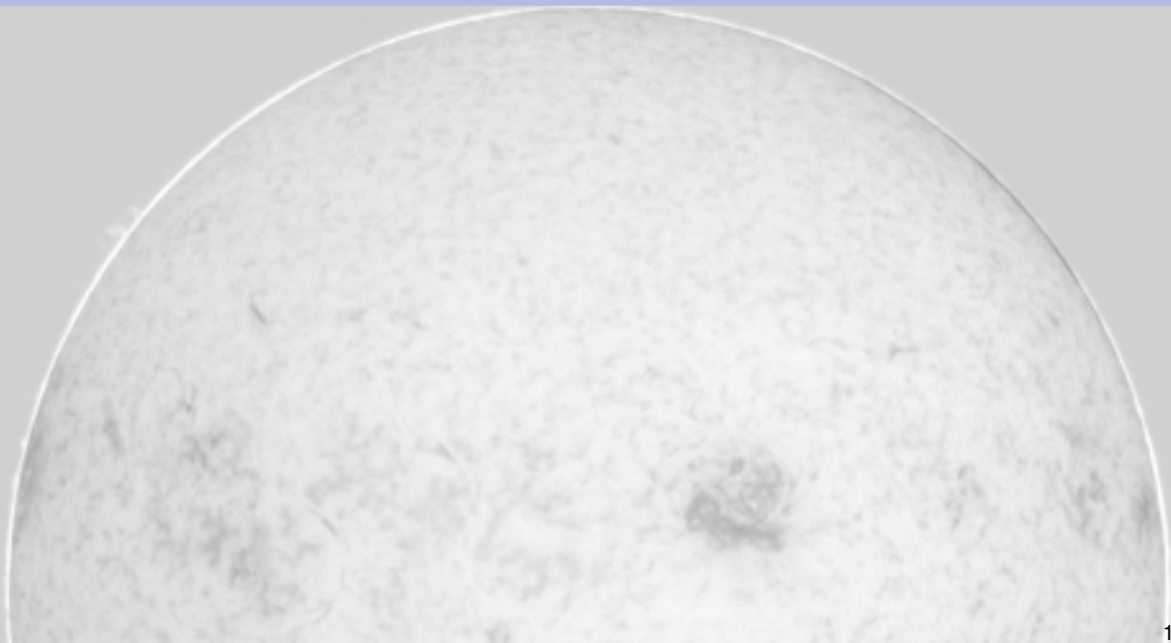
## Scientific future of He I 10830

## To-Do list for He I 10830 Science

- obtain measurements at highest possible spatial resolution, S/N in the low  $10^{-4}$  range (ideal: 2D FOV)
- reliable disambiguation methods (Van Vleck ambiguity,  $180^\circ$  Hanle & Zeeman ambiguity):  
→ combination with other chromospheric line?
- reliable anisotropy determination (take into account coronal illumination, symmetry breaking due to, e.g., sunspots):  
→ determine population imbalances
- reliable height determination: → high S/N, stereoscopy

# Bibliography

- Asensio Ramos, A., Trujillo Bueno, J., & Landi Degl'Innocenti, E. 2008, *ApJ*, 683, 542
- Avrett, E. H., Fontenla, J. M., & Loeser, R. 1994, in IAU Symp. 154: Infrared Solar Physics, ed. Rabin, D. M. (Kluwer Academic Publishers, Dordrecht, 1994), 35–47
- Bethge, C., et al. 2011, *A&A*, 534, A105
- Bommier, V., et al. 1994, *Sol. Phys.*, 154, 231
- Cao, W., et al. 2012, in Astronomical Society of the Pacific Conference Series, Vol. 463, Second ATST-EAST Meeting: Magnetic Fields from the Photosphere to the Corona., ed. Rimmele, T. R., et al., 291
- Casini, R., et al. 2003, *ApJL*, 598, L67
- Centeno, R., et al. 2008, *ApJ*, 677, 742
- Collados, M., et al. 2007, in Astronomical Society of the Pacific Conference Series, Vol. 368, The Physics of Chromospheric Plasmas, ed. Heinzel, P., Dorotovič, I., & Rutten, R. J., 611
- Collados, M., et al. 2012, *Astronomische Nachrichten*, 333, 872
- Collados, M., et al. 1999, in *Astronomische Gesellschaft Meeting Abstracts*, 13–+
- Elmore, D. F., et al. 2008, in Society of Photo-Optical Instrumentation Engineers (SPIE) Conference Series, Vol. 7014, Society of Photo-Optical Instrumentation Engineers (SPIE) Conference Series, 16
- Hanaoka, Y., et al. 2011, in *Astronomical Society of the Pacific Conference Series*, Vol. 437, Solar Polarization 6, ed. Kuhn, J. R., et al., 371
- Jaeggli, S. A., et al. 2010, *Memorie della Societa Astronomica Italiana*, 81, 763
- Ji, H., Cao, W., & Goode, P. R. 2012, *ApJL*, 750, L25
- Keller, C. U., Harvey, J. W., & Giampapa, M. S. 2003, in Society of Photo-Optical Instrumentation Engineers (SPIE) Conference Series, Vol. 4853, Innovative Telescopes and Instrumentation for Solar Astrophysics, ed. Keil, S. L. & Avakyan, S. V., 194–204
- Lagg, A., et al. 2009, in *Astronomical Society of the Pacific Conference Series*, Vol. 415, The Second Hinode Science Meeting:
- Beyond Discovery-Toward Understanding, ed. Lites, B., et al., 327
- MacQueen, R. M., et al. 1998, *Sol. Phys.*, 182, 97
- Martínez Pillet, V., et al. 1999, in *Astronomische Gesellschaft Meeting Abstracts*, 5–+
- Orozco Suárez, D., Asensio Ramos, A., & Trujillo Bueno, J. 2014, *A&A*, 566, A46
- Schad, T. A. 2013, PhD thesis, The University of Arizona
- Schad, T. A., Penn, M. J., & Lin, H. 2013, *ApJ*, 768, 111
- Shibata, K., et al. 2007, *Science*, 318, 1591
- Socas-Navarro, H., et al. 2006, *Sol. Phys.*, 235, 55
- Trujillo Bueno, J. 2001, in *ASP Conf. Ser.* 236: Advanced Solar Polarimetry – Theory, Observation, and Instrumentation, 161
- Vargas Domínguez, S., Kosovichev, A., & Yurchyshyn, V. 2014, *ApJ*, 794, 140
- Vissers, G. & Rouppe van der Voort, L. 2012, *ApJ*, 750, 22

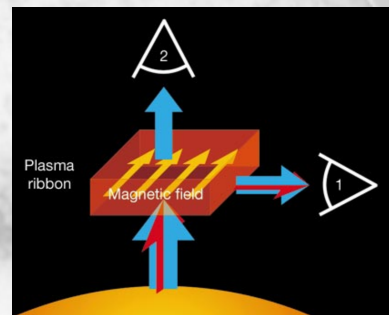
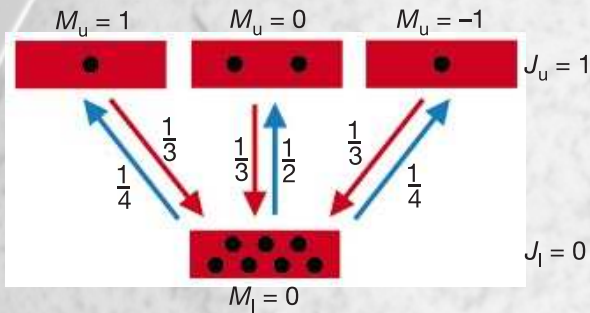


## Atomic Polarization (Trujillo Bueno, 2001)

### Case 1: $J_{\text{lower}} = 0 \rightarrow J_{\text{upper}} = 1$

“normal” (scattering) case: upper level atomic polarization

- polarization only in emission (1) (90° scattering)
- no polarization in absorption (2) (forward scattering)

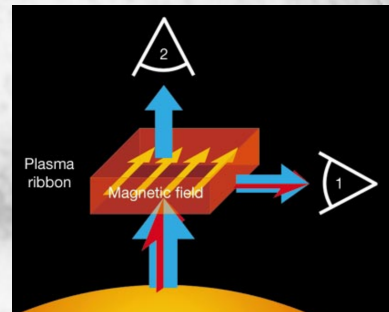
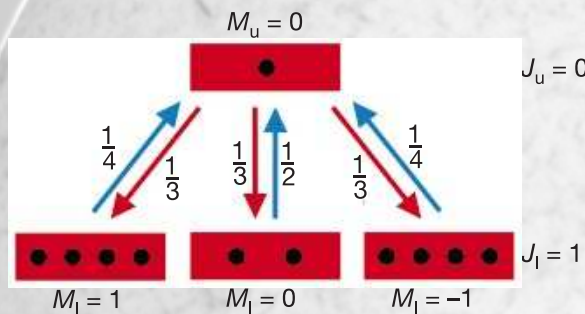


## Atomic Polarization (Trujillo Bueno, 2001)

Case 2:  $J_{\text{lower}} = 1 \rightarrow J_{\text{upper}} = 0$

degenerate lower level: upper level cannot carry atomic polarization

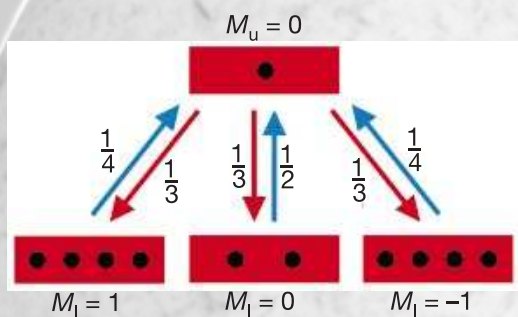
- emitted beam (1) unpolarized
- polarization of transmitted beam (2) depends on “uneven” population of lower level



## Case 2: $J_{\text{lower}} = 1 \rightarrow J_{\text{upper}} = 0$

degenerate lower level: upper level cannot carry atomic polarization

- emitted beam (1) unpolarized
- polarization of transmitted beam (2) depends on “uneven” population of lower level



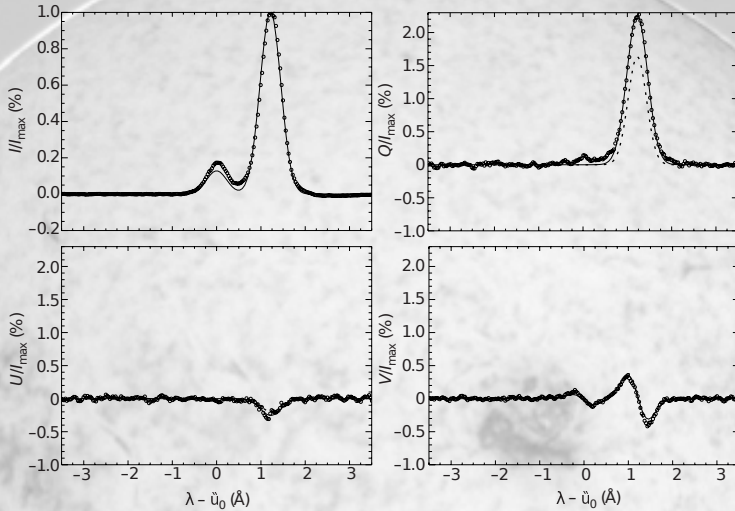
$J_u = 0$  blue component of He I line  
lower level carries atomic polarization

Plasma

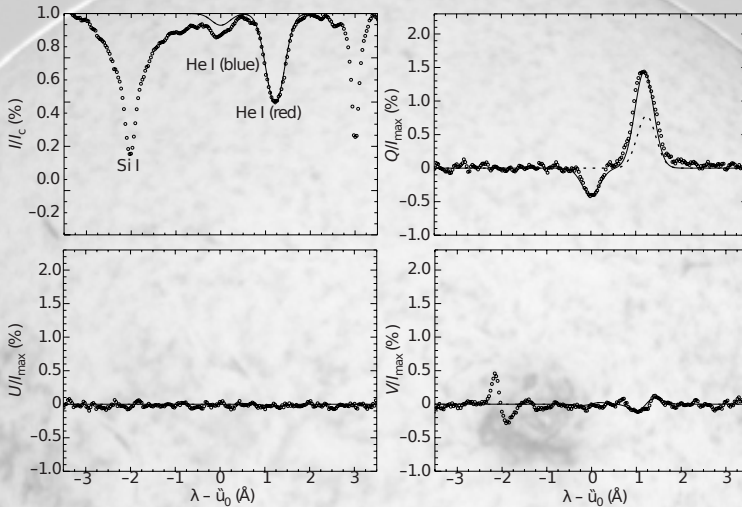
red components of He I line

$J_l = 1$  both levels carry atomic polarization

# Atomic Polarization: Emission Profiles (Trujillo Bueno, 2001)



# Atomic Polarization: Absorption Profiles (Trujillo Bueno, 2001)



## He I: From milli-Gauss to kilo-Gauss

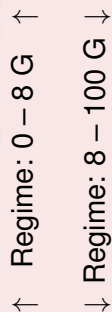
## Hanle sensitive region

linear polarization signal  
depends on:

- ❶ magnetic field strength
  - ❷ magnetic field direction

around  $B = 10^{-2}$  G, the density matrix elements start to be affected by the magnetic field caused by a feedback effect that the alteration of the lower-level polarization has on the upper levels

Application: very weak fields  
(high S/N required!)



Zeeman:  
 $>70$  G

## Hanle saturation regime

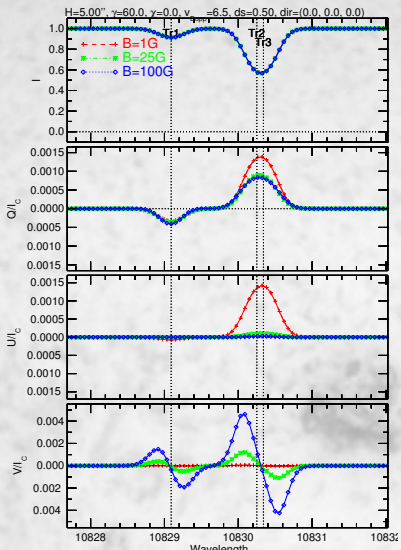
linear polarization signal  
depends on

- ## ① magnetic field direction

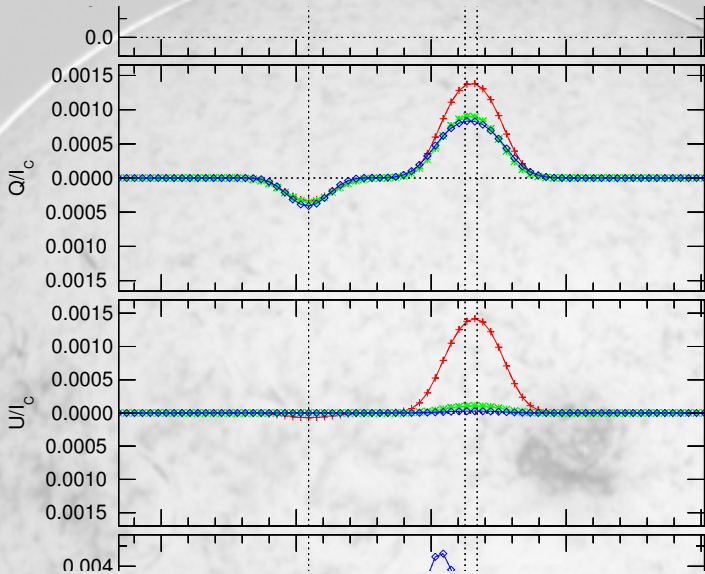
coherences are negligible and the atomic alignment values of the lower and upper levels are insensitive to the strength of the magnetic field

Application:  
disk center, horizontal field:  
 $\tan(2\phi) = Q/U$

# Atomic Polarization Causes Linear Polarization



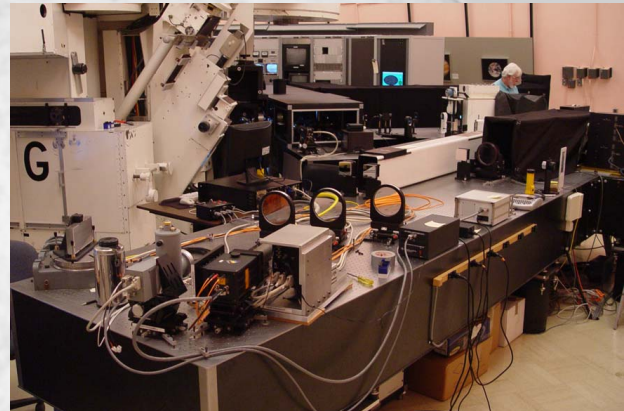
# Atomic Polarization Causes Linear Polarization



Spectro-POlarimeter for  
INfrared and Optical Regions  
SPINOR (Socas-Navarro et al.,  
2006)

- full Stokes simultaneous observation of several VIS + IR regions
- virtually any combination of spectral line

Detector: Rockwell TCM 8600  
slit length: 120"

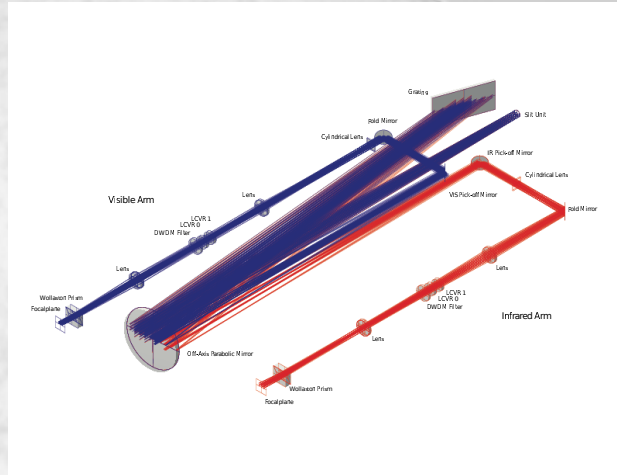


## FIR@ DST (Sac Peak)

Facility Infrared  
Spectrapolarimeter FIRS  
(Jaeggli et al., 2010; Schad,  
2013)

- 4-slit, dual-beam spectropolarimeter
- Fe I 630.2 & He I 1083
- simultaneous with IBIS

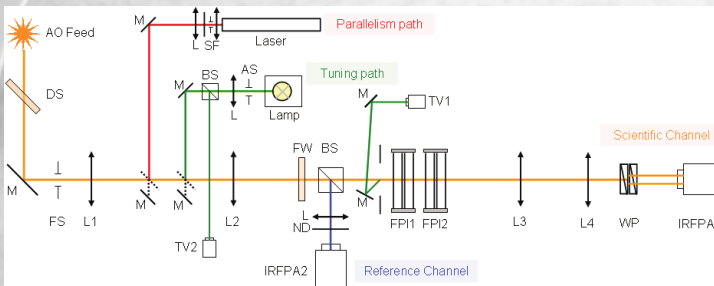
Det: Raytheon Virgo 1k×1k HgCdTe  
@He I:  $\lambda/\Delta\lambda > 3.5 \cdot 10^5$ , 0.''36  
FOV: 174''×75'' in 18 min  
S/N: 1000 in 7.5 s



# NIRIS @ 1.6m NST (Big Bear)

## Near-InfraRed Imaging Spectropolarimeter NIRIS (Cao et al., 2012)

- attached to 1.6 m NST at Big Bear
- dual Fabry-Pérot Interferometers
- $2 \times 2k$  HgCdTe HAWAII-2RG



Wavelength range:  
1000–1700 nm

Spectral resolving power:  
 $\lambda/\Delta\lambda = 1.0–1.5 \cdot 10^5$

FOV: 85 arcsec

Parasitic light:  $< 10^{-3}$

Spatial sampling:  
0.083 arcsec/pixel<sup>-1</sup>

Exposure time:  
20 ms for S/N  $\geq 400$

Strehl ratio:  $\geq 0.7$

Zeeman sensitivity:  
 $\approx 10^{-4} I_c$

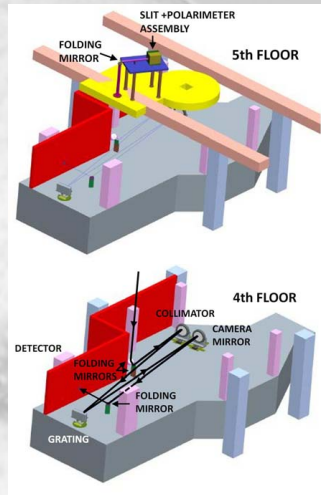
Spectroscopy:  
< 1 s cadence

Vector spectro-polarimetry:  
< 10 s cadence

## GREGOR Infrared Spectrograph (Collados et al., 2012)

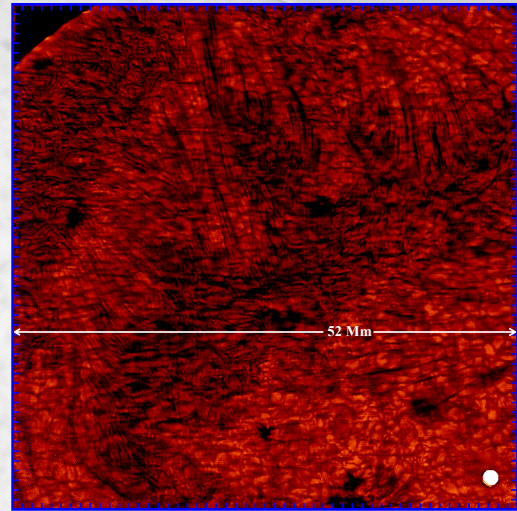
- attached to 1.5 m GREGOR telescope (Tenerife)
- standard Czerny-Turner configuration
- $1 \times 1\text{k}$  HgCdTe Rockwell TCM 8600

Wavelength range:	1000–2300 nm
Spectral resolving power:	$\lambda/\Delta\lambda = 1.9 \cdot 10^5$
FOV:	65 arcsec
Spatial sampling:	0.126 arcsec/pixel <sup>-1</sup>
Zeeman sensitivity:	$\approx 10^{-4} I_c$
Spectroscopy:	< .1 s cadence
Vector spectro-polarimetry:	< 2 s cadence

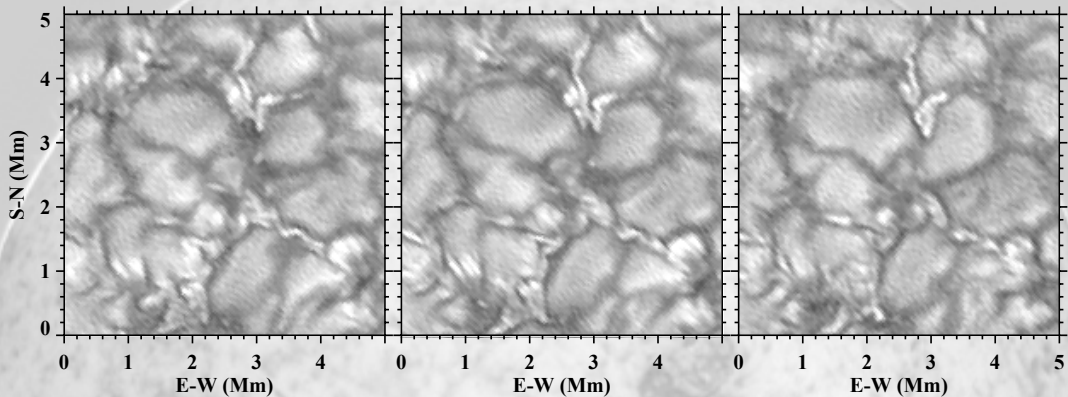


### NST IRIM in He I 10830

- unexpected complexes of ultrafine loops (100 km) reaching from photosphere to base of corona
- origin: intense, compact magnetic field elements in intergranular lanes
- He I absorbing material injections with subsequent coronal brightening (observed in AIA/SDO loops)

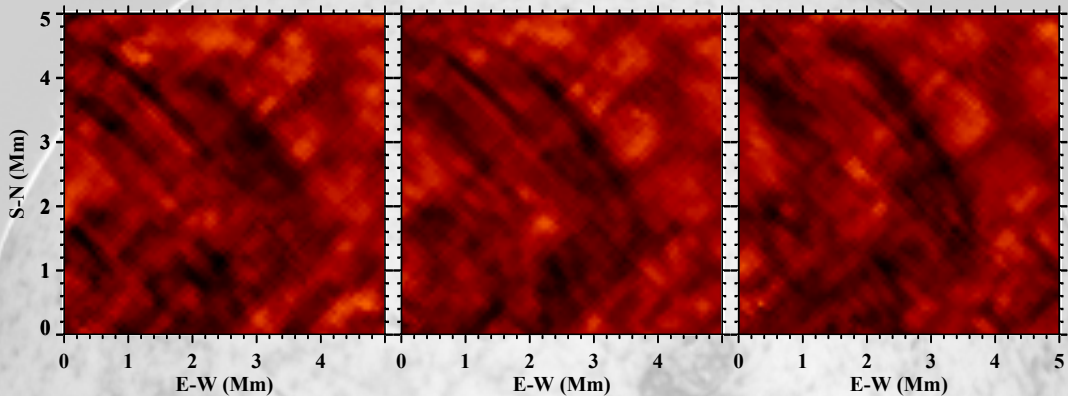


## Observation of Ultrafine Channels of Solar Corona Heating (Ji et al., 2012)



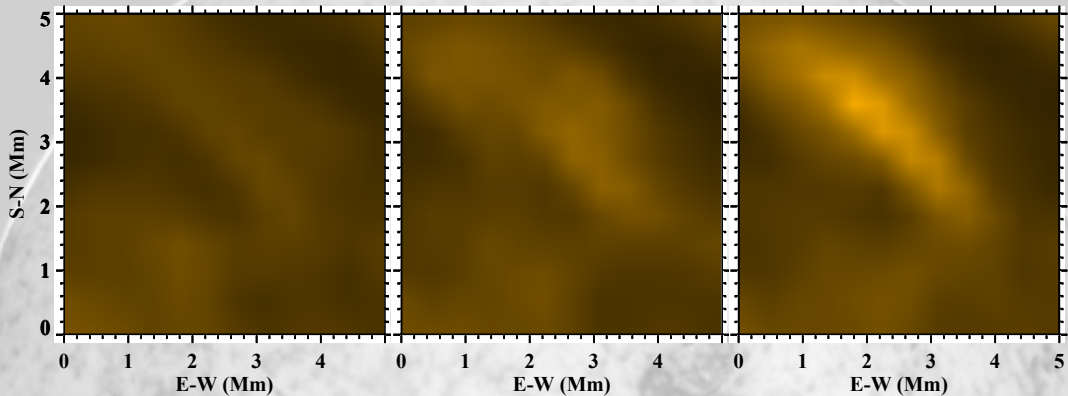
TiO 7057 Å

## Observation of Ultrafine Channels of Solar Corona Heating (Ji et al., 2012)



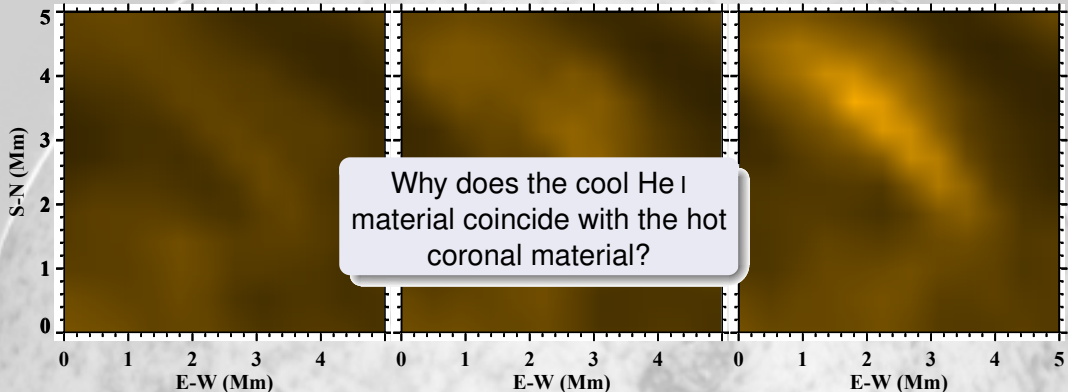
He I 10830 Å

## Observation of Ultrafine Channels of Solar Corona Heating (Ji et al., 2012)

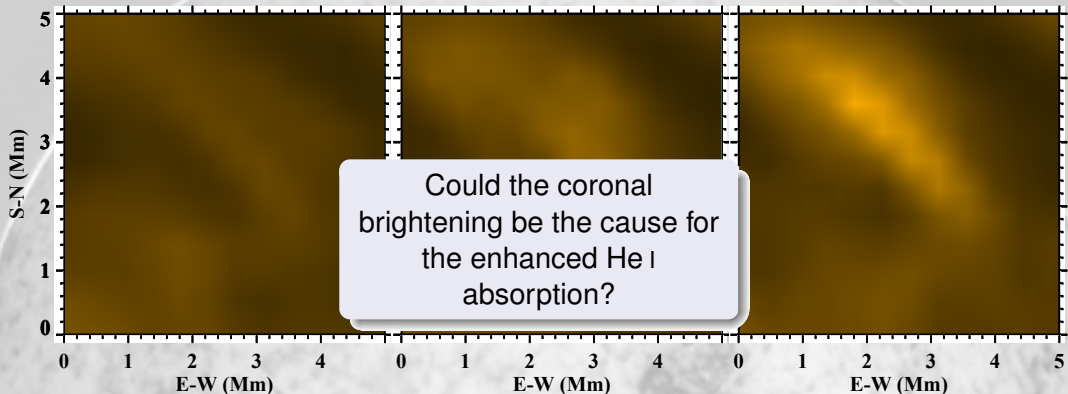


AIA 171 Å

## Observation of Ultrafine Channels of Solar Corona Heating (Ji et al., 2012)



## Observation of Ultrafine Channels of Solar Corona Heating (Ji et al., 2012)



AIA 171 Å

## Observation of Ultrafine Channels of Solar Corona Heating (Ji et al., 2012)

